

Article

The Antifungal Properties of Super-Hydrophobic Nanoparticles and Essential Oils on Different Material Surfaces

Monika Benkovičová ¹, Zuzana Kisová ², Mária Bučková ², Eva Majková ^{1,3}, Peter Šiffalovič ^{1,3} 
and Domenico Pangallo ^{2,*} 

¹ Institute of Physics, Slovak Academy of Sciences, Dúbravská cesta 9, Sk-84511 Bratislava, Slovakia; monika.benkovicova@savba.sk (M.B.); eva.majkova@savba.sk (E.M.); peter.siffalovic@savba.sk (P.S.)

² Institute of Molecular Biology, Slovak Academy of Sciences, Dúbravská cesta 21, SK-84551 Bratislava, Slovakia; zuzana.kisova@savba.sk (Z.K.); maria.buckova@savba.sk (M.B.)

³ Center for Advanced Material Application, Slovak Academy of Sciences, Dúbravská cesta 9, Sk-84511 Bratislava, Slovakia

* Correspondence: domenico.pangallo@savba.sk

Received: 7 February 2019; Accepted: 1 March 2019; Published: 6 March 2019



Abstract: This study was undertaken to determine the in vitro antifungal activities of super-hydrophobic nanoparticles (SHNPs), essential oils (EOs), and their mixtures (SHNPs/EOs). We have applied a thin layer of SHNPs in combination with various concentrations of three EOs: Arborvitae (*Thuja plicata*), Oregano (*Origanum vulgare* L.), and Thyme (*Thymus vulgaris*). The mixtures were spread on the surface of different materials: whitewood, sandstone, and paper. The antifungal and protective properties of these SHNP and EO mixtures were evaluated. The parameter R_r (ratio of reflectivity) was determined to identify the color changes of substrates. Digital microscopy was used to measure the colonization area of molds and also their penetration in the analyzed materials. Surprisingly, the use of SHNPs alone showed a balanced compromise in order to inhibit the mold growth on assayed surfaces.

Keywords: super-hydrophobic nanoparticles; essential oils; fungi; antifungal activity; growth inhibition; penetration

1. Introduction

The super-hydrophobic nanoparticles (SHNPs) can self-assemble and form the superhydrophobic surfaces with hierarchical, micro-, and nano-scale roughness [1–4]. The superhydrophobic surface is defined as the one with a water contact angle larger than 150° [5]. Air trapped in the roughness reduces the effective contact area on the liquid/solid interface and can give rise to very large contact angles of up to 177° [1]. Those extremely water-repellent surfaces are scientifically interesting in many applications, including self-cleaning surfaces, in the automotive and aircraft industry (drag reduction), as well as in preparation of special coating materials for antimicrobial applications [6].

Plant extracts and secondary metabolites, such as essential oils, tannins, alkaloids, and flavonoids, have been reported to have promising fungicidal activities [7–9]. Essential oils (EOs) are complex mixtures comprising many compounds. A number of studies have been performed in order to determine the antimicrobial activity of many essential oils, including those from oregano, thyme, and arborvitae [9,10]. Their strong antimicrobial activity could be used as a natural safe protection of material surfaces, for example the arborvitae EO have been traditionally used as a natural insect repellent and wood preservative [11,12]. Oregano and thyme EOs are able to inhibit growth of pathogenic microorganisms [13,14].

Molds are ubiquitously distributed in nature and their spores can be found in the atmosphere even at high altitudes, carried and disseminated by wind and air currents, as well as can be spread by insects and animals [15]. The metabolic activities accompanying the growth and mold development decompose organic substrates, and because of their powerful arsenal of hydrolytic enzymes, molds are responsible for the deterioration of several materials [16,17].

Aspergillus fumigatus has lignocellulolytic abilities [18], as well as its presence on various types of historical documents having been detected [19]. They also belong to the group of indicator microorganisms typical of moisture-damaged buildings [20,21].

Another type of fungus is *Exophiala xenobiotica*, so-called black yeasts. The members of this genus belonged to the slow-growing rock-inhabiting microfungi group [22]. The occurrence of this fungus on the stones is reported to be combined with unaesthetic spoiling due to color changes, such as patina or black spots. There is strong evidence that these microorganisms are able to colonize deeper cracks, and induce crater shaped lesions that leads to chipping and exfoliation of the rock surface combined with the loss of materials. These fungi belong to major agents of microbial deterioration of building stones, such as marble, granite, sandstone, and mortars [23]. For this reason, many efforts are spent to remove the already established microbial community, and to some extent to reduce the rate of recolonization [24–27].

Our study is focused on the fungi *A. fumigatus* and *E. xenobiotica*, which are responsible for the deterioration of several materials. This paper deals with the evaluation of the antifungal effect against the abovementioned fungi, of three EOs (arborvitae, oregano, and thyme) and various mixtures of SHNPs with these selected EOs in varying concentrations. The SHNPs are able to create a superhydrophobic surface that could provide a barrier to limit the fungal growth on the surface or in the structure of the material. In this way we suppose to improve the antifungal effect of EOs.

Here, the surface functionalization of commercial silica nanoparticles with octadecyltrichlorosilane was used to prepared SHNPs according to Siffalovic et al [5]. To monitor the antifungal effect, the EOs and EO/SHNP mixtures were used to treat sandstone, whitewood, and paper. The antifungal and optical properties on the surfaces of selected materials were evaluated using digital optical microscopy and UV/Vis/NIR (Ultraviolet–Visible–Near-Infrared) spectrophotometry.

2. Materials and Methods

2.1. Superhydrophobic Nanoparticles

Aerosil fumed silica was purchased from Evonik (Hanau-Wolfgang, Germany), and toluene (anhydrous, 99.8%) and octadecyltrichlorosilane (OTS, 90%) from Sigma Aldrich (Bratislava, Slovakia). Aerosil fumed silica (1.5 g) was annealed in a beaker at 120 °C for 24 h. After annealing, the aerosil was dissolved in toluene (50 mL) and functionalized with an organic surfactant OTS (2 g). The reaction took place while stirring the solution at a temperature of 50 °C for 24 h. The functionalized particles were centrifuged 3-times in toluene to remove the unbound surfactant. The final particles were dried at 150 °C for 5 h and dispersed in chloroform at a concentration of 0.1 mg/mL. Whole reaction (annealing and functionalization) was carried out in a glove box under argon atmosphere. The size of SHNPs is 14 nm in diameter with a specific surface area of $150 \pm 15 \text{ m}^2/\text{g}$.

The water contact angle of SHNPs and SHNP/EO mixtures was measured on silicon wafer, wood, and sandstone substrates by a sessile drop-shape method, using KSV CAM 200 (KSV Instruments, Helsinki, Finland).

2.2. Essential Oils

Arborvitae, oregano, and thyme essential oils were supplied by dōTERRA International LLC company ((Pleasant Grove, UT, USA). The main constituents are: arborvitae, *methyl thujate*; oregano, *carvacrol*, *thymol*; thyme, *thymol*, *para-cymene*, *γ-terpinene*. The producer guarantees the chemical composition of each EO based on gas chromatography–mass spectrometry (GC/MS) analysis.

For experiments, the oils were diluted in ethanol (99.9%, Merck; Darmstadt, Germany) in concentrations of 10, 30, and 50%.

2.3. Antifungal Ability of SHNPs and SHNP/EO Mixtures: Disc Diffusion Assay

Saprotroph *A. fumigatus*, obtained from achistorical paper document [19], and *E. xenobiotica*, isolated from soil, were used in the experimentation.

It was applied by the same approach proposed by Puškárová et al [9]. Briefly, conidia suspensions (*A. fumigatus* and *E. xenobiotica*) were adjusted using a Neubauer's chamber to 10^6 conidia per mL. Then, 300 μ L of each fungal suspension was applied to Malt Extract Agar (MEA; Himedia, Mumbai, India) plates. Filter paper discs (6 mm diameter; Whatman No.1) were placed on the agar surface of the Petri dishes and each mixture SHNPs and EOs, dissolved in ethanol at different concentrations (50, 30, and 10%) of EOs, was individually added. For each dilution, the same volume as the full-strength sample was placed on the sterile disc.

Discs impregnated with 10 μ L of ethanol were used as controls. Petri dishes were incubated at 26 °C for 5 days. Inhibition zone diameters were measured in mm. An inhibition zone larger than 1 mm was taken to indicate a positive effect. The assays were performed in triplicate.

2.4. Antifungal Ability of SHNPs and SHNP/EO Mixtures on Selected Materials

For laboratory experimentation, sandstone, whitewood, and Whatman filter paper (Munktell, Falun, Sweden) were cut into rectangular units. The size of these units were approximately 30 mm long and 20 mm wide; sandstone and whitewood samples were also 10 mm deep. All sides of materials were exposed to UV irradiation (UVC-508 UV crosslinker, Ultra-Lum, Inc.; Paramount, CA, USA) for 10 min.

After UV disinfection, 200 μ L of EOs in ethanol and mixture of EOs/SHNPs (200 μ L of SHNPs in chloroform and 200 μ L EOs in ethanol) were applied by micropipette to whole surface of sandstone and whitewood plate, while 100 μ L was applied to paper. In the case of the mixture of EOs/SHNPs application, the EOs were applied as a final coating of material when the chloroform was evaporated from the surface of substrates after treatment with SHNPs.

2.5. Application of Fungal Strains on the Surface of Selected Materials

Fungal strains were cultivated on MEA at 28 °C. After growth, the fungi were suspended in a physiological solution (pH 7.2) to obtain a concentration of 10^6 spores/ml. Two-hundred μ L of this suspension was used to inoculate sandstone, whitewood, and paper in the center of the surface. The incubation period was one month at 28 °C. According to the environment of isolation of the fungi, *Aspergillus fumigatus* was inoculated on whitewood and paper, while *Exophiala xenobiotica* was used on sandstone (Figure S1).

2.6. Measurement of Antifungal Activities

The antifungal activities (localized fungal area on surface and penetration depth of fungi into material) of the EOs and EO/SHNP mixtures on the above-mentioned materials were monitored on their surfaces and in the cross-section after the incubation period (one month) by digital optical microscopy with a long working distance zoom objective (Keyence, Osaka, Japan). The penetration depth of fungi into the material was analyzed only for whitewood samples. In terms of paper thickness and sandstone structure, it was not possible to determine the exact penetration depth of fungi into these materials.

2.7. Measurement of Optical Properties

The spectral reflectivity measurements took place in SolidSpec-3700 UV-VIS-NIR spectrophotometer from Shimadzu (Kyoto, Japan). It is a grating type double monochromator that uses and automatically

switches between a total of four blazed holographic diffraction gratings (type Shimadzu), depending on the wavelength. The pre-monochromator is equipped with two concave diffraction gratings (1000 and 250 lines/mm) and the main monochromator is a Czerny-turner type with two flat diffraction gratings (1200 and 300 lines/mm). The photometric system is a double beam, direct ratio measuring system, and the light sources were a deuterium and halogen lamp (50 W) used with automatic position alignment. The geometry of diffuse reflection measurement using an integrating sphere is shown in Figure S2. The integrating sphere is equipped with three detectors: a photomultiplier, InGaAs, and PbS. The slit width was set to 32 nm during the measurements. Spectra were recorded in the range: 200–1000 nm. The Baseline correction prior to reflectivity measurement was performed using a standard white plate composed of BaSO₄.

3. Results and Discussion

To our knowledge, in this study the protection ability of SHNPs/EOs combination was evaluated for the first time. Firstly, the antifungal properties of SHNPs and the combination SHNPs/EOs were assessed using a disc diffusion assay. The SHNPs alone did not display any antifungal properties. The growth inhibition of *A. fumigatus* and *E. xenobiotica* was displayed when the mixtures, SHNPs/EOs, were assayed. Generally, the degree of fungal inhibition was directly dependent on the amount of EOs; the greatest percentage of EOs produced the largest inhibition zone (Table 1; Figures S3 and S4). The combination of SHNPs and oregano was the most effective one.

Table 1. Antifungal activity of different combinations of EOs and SHNPs.

	<i>A. Fumigatus</i> *	<i>E. Xenobiotica</i> *
SHNPs	-	-
SHNPs/Oregano 10%	20	18
SHNPs/Oregano 30%	22	20
SHNPs/Oregano 50%	30	30
SHNPs/Thyme 10%	15	10
SHNPs/Thyme 30%	22	12
SHNPs/Thyme 50%	25	20
SHNPs/Arborvitae 10%	10	10
SHNPs/Arborvitae 30%	20	15
SHNPs/Arborvitae 50%	22	20

* Mean of zone inhibition (diameter) in mm; -: no inhibition.

We have checked the water contact angles of the EOs, SHNPs, and SHNP/EO mixtures on each surface (Figure S5). In some cases, the water contact angles were not detected due to the wettability of the surface (EOs of 10% on whitewood and sandstone, EOs on paper). Usually, the high values were obtained with the SHNPs alone or with the mixtures with 10% of EOs. The water contact angles decreased with the increasing amount of EOs for the mixtures on both whitewood and sandstone (Table 2). It indicates that the increasing percentage of EOs has a negative influence on the hydrophobic properties of the coating film (SHNPs/EOs). These results have a certain similarity with previous research, where the contact angle, and consequently also the hydrophobicity, decreased when whitewood was treated with thyme EOs [28]. On the contrary, the hydrophobicity increased with an increasing percentage of the oil in the mixture of SHPs/EOs on the paper surface. For some authors [29,30], a surface is hydrophobic if the contact angle is greater than 65°, but in general, a surface is hydrophobic when its water static contact angle is >90°, while angles <90° reveal hydrophilic surfaces [31]. The values greater than 65° were measured mainly on sandstone samples (Table 2). In available literature, we did not find any data concerning the contact angle measurements of SHNP/EO mixtures, hence our findings can be considered as novel.

Table 2. Contact angle measurements of EOs, SHNPs, and SHNP/EO mixtures on different material surfaces.

Untreated Samples					
Material			Contact angle (°)		
Whitewood			-		
Sandstone			-		
Paper			-		
Treated samples					
Silicon wafer with SHNPs			171.10 ± 1.50		
Whitewood		Sandstone		Paper	
EOs and mixtures	Contact angle (°)	EOs and mixtures	Contact angle (°)	EOs and mixtures	Contact angle (°)
A 10%	-	A 10%	-	A 10%	-
A 30%/	35.59 ± 2.04	A 30%/	42.13 ± 3.55	A 30%/	-
A 50%	49.51 ± 2.68	A 50%	49.95 ± 3.55	A 50%	-
O10%	-	O10%	-	O 10%	-
O 30%	34.84 ± 1.28	O 30%	42.15 ± 4.06	O 30%	-
O 50%	38.53 ± 4.88	O 50%	43.46 ± 2.59	O 50%	-
T 10%	-	T 10%	-	T 10%	-
T 30%	36.15 ± 3.17	T 30%	48.84 ± 3.89	T 30%	-
T 50%	50.43 ± 2.94	T 50%	44.47 ± 2.85	T 50%	-
SHNPs	124.14 ± 11.89	SHNPs	106.32 ± 14.37	SHNPs	115.58 ± 2.87
A 10%/SHNPs	91.08 ± 8.16	A 10%/SHNPs	100.95 ± 16.23	A 10%/SHNPs	-
A 30%/SHNPs	66.63 ± 4.44	A 30%/SHNPs	98.92 ± 10.57	A 30%/SHNPs	69.92 ± 3.73
A 50%/SHNPs	59.17 ± 2.93	A 50%/SHNPs	72.38 ± 8.96	A 50%/SHNPs	85.92 ± 1.55
O 10%/SHNPs	129.05 ± 40.77	O10%/SHNPs	108.03 ± 13.27	O 10%/SHNPs	-
O 30%/SHNPs	73.22 ± 4.52	O 30%/SHNPs	70.77 ± 2.33	O 30%/SHNPs	-
O 50%/SHNPs	55.34 ± 5.76	O 50%/SHNPs	71.57 ± 4.85	O 50%/SHNPs	72.50 ± 2.87
T 10%/SHNPs	66.58 ± 8.25	T 10%/SHNPs	133.68 ± 26.33	T 10%/SHNPs	-
T 30%/SNHPs	65.19 ± 4.86	T 30%/SNHPs	84.08 ± 2.99	T 30%/SNHPs	71.98 ± 2.07
T 50%/SHNPs	62.05 ± 7.03	T 50%/SHNPs	95.90 ± 11.88	T 50%/SHNPs	98.49 ± 1.11

Note: A = arborvitae; O = oregano; T = thyme; “-” mean immeasurable water contact angle.

The mixtures of SHNPs and EOs have to protect the materials against molds, but they should also preserve the material’s characteristics, such as appearance and color. A good way to determine the color change of a material is to measure the integral surface reflectivity, which includes the diffuse and specular reflectivity components. First, we measured the reflectivity of clean substrates (without coating of SHNPs/EOs) and subsequent reflectivity after deposition of the SHNPs, Eos, and their mixtures. To emphasize the spectral reflectivity changes after layer application, we introduced the reflectivity ratio parameter R_r in visible spectral region (400–700 nm), as follows

$$R_r = \frac{R_{(\text{coating})}}{R_{(\text{substrate})}}, \quad (1)$$

where R_{coating} is reflectivity after application of the layer on the substrate and $R_{\text{substrate}}$ is reflectivity of the clean substrate.

Figure 1 shows the R_r values on the whitewood plates. Parameter R_r was calculated for all sample types and for all concentrations (10%, 30%, and 50%) of arborvitae (A), oregano (O), and thyme oil (T), with or without SHNPs. In the cases of whitewood samples coated only with EOs (without SHNPs), the deviations from the original reflectance of the clean uncoated substrate have increased in the following order: A, O, T 10% < A, O, T 30% < A, O, T 50%. The general trend for all surfaces with applied EOs is a decreased substrate reflectivity in the blue-green part of the visible spectrum due to a substantial absorption cross-section of EOs in the UV spectral region. The R_r parameter for the lowest concentration was close to 1, which means that using a 10% solution of EOs does not considerably alter the color appearance of the treated surface for naked eye observation.

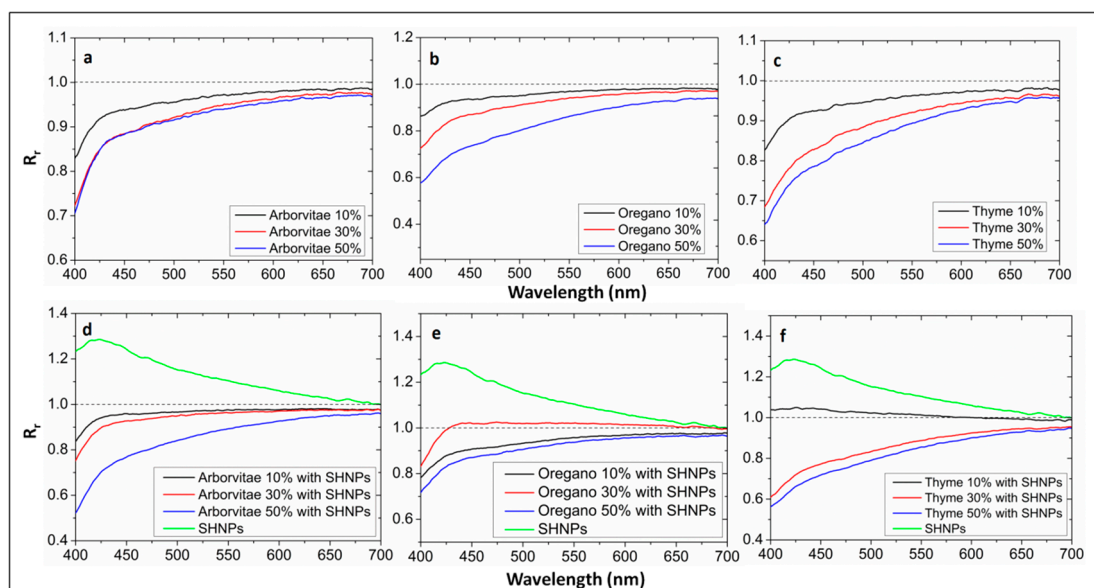


Figure 1. Dependence of the reflectivity ratio R_r as a function of wavelength for whitewood samples. (a) 10%, 30%, 50% Arborvitae EO; (b) 10%, 30%, 50% oregano EO; (c) 10%, 30%, 50% Thyme EO; (d) 10%, 30%, 50% Arborvitae EO with SHNPs; (e) 10%, 30%, 50% Oregano EO with SHNPs; (f) 10%, 30%, 50% Thyme EO with SHNPs.

On the other hand, after deposition of SHNPs onto a clean substrate, we observed a significant reflectivity increase in the blue-green part of the visible spectrum when compared to uncoated samples. This observation can be understood in terms of increasing the Rayleigh scattering cross-section ($\sim \lambda^{-4}$) of SHNPs towards the UV spectral region. This result suggests that the application of SHNPs can mitigate the undesirable absorption of EOs in the blue-green spectral region. This was validated for coatings of SHNPs with 10% of EOs. Only small deviations of R_r parameters in the violet part of the visible spectra, close to 400 nm, suggest nearly unchanged color appearance of supporting substrates. To summarize, when the substrates with SHNP layers were coated by EOs, the reflectance was reduced in the following order: A, T with SHPs 10% > 30% > 50%. This order was not confirmed for oregano oil. This is probably due to the fact that the substrates where oregano oil was applied have larger deviations in surface roughness, which results in a different penetration depth into the substrate structure.

The same procedure was used for the sandstone samples as well (Figure 2). The absence of lowered blue-green reflectivity of sandstone samples when compared to whitewood can be ascribed to the high capillary absorption of sandstone towards EOs due to its intrinsic porosity. However, saturation of the sub-surface pores of sandstone was observed for some samples, especially for the sandstone samples treated with 50% of arborvitae EO. Deviations from original reflectance of the pure sandstone have increased in the same order as the whitewood samples, except for 30% and 50% thyme. This discrepancy can be related to the difference in porosity between various samples, which contributes to a different penetration depth of oil into the bulk structure of sandstone. However, the samples with oregano oil of concentration of 10% and 30% showed a minimal change in reflectivity when compared to the pristine substrate.

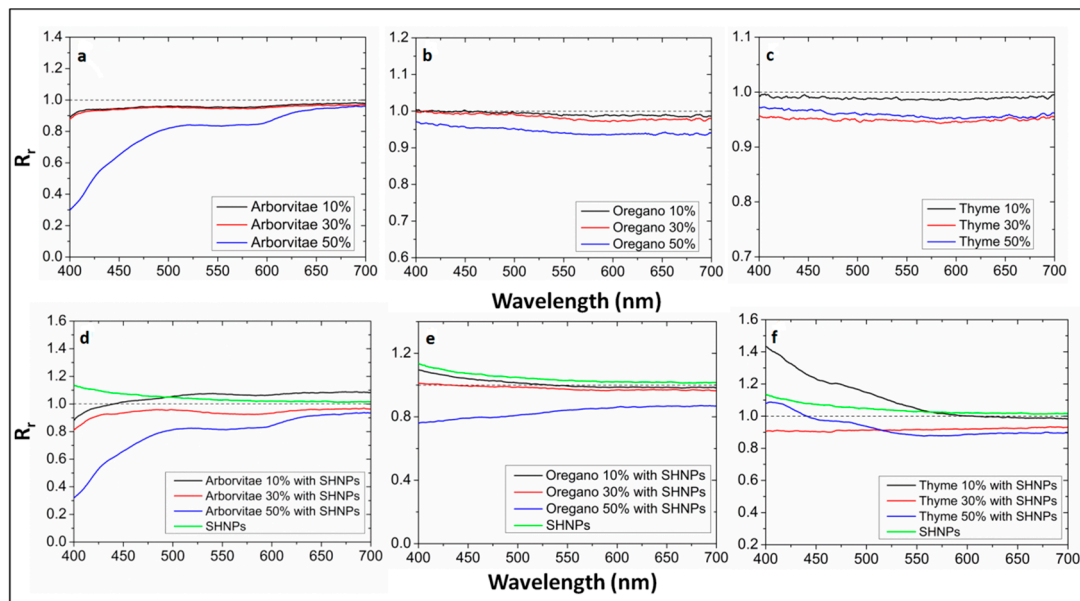


Figure 2. Dependence of the reflectance ratio R_r as a function of wavelength for sandstone samples. (a) 10%, 30%, 50% Arborvitae EO; (b) 10%, 30%, 50% oregano EO; (c) 10%, 30%, 50% Thyme EO; (d) 10%, 30%, 50% Arborvitae EO with SHNPs; (e) 10%, 30%, 50% Oregano EO with SHNPs; (f) 10%, 30%, 50% Thyme EO with SHNPs.

The application of SHNPs has identical influence on the spectral reflectivity, as in the case of whitewood. The enhanced Rayleigh scattering cross-section of SHNPs for smaller wavelengths increases the reflectivity of sandstone samples in the blue part of the visible light spectrum. The high vapor pressure of chloroform solvent used in application of SHNPs contributes to significantly reduced capillary absorption of SHNPs into the bulk structure of sandstone. Due to this fact the SHNPs were trapped on the surface and in sub-surface regions of sandstone, and hence contributed to its enhanced reflectivity in blue part of visible spectrum. The samples coated with SHNPs/EOs layer decreased in reflectivity in the order of increasing concentration of EOs. The reflectance values fluctuated significantly for arborvitae oil with SHNPs, but in the case of 50% arborvitae oil with SHNPs, the reflectance was very similar to the sample prepared by 50% oil without SHNPs. The best results in terms of unchanged reflectivity for the sandstone samples were achieved when oregano oil was used. There was a minimum difference in spectral reflectivity before and after coating application.

The reflectivity results confirmed that the R_r values are intimately correlated with the characteristics of the surface of two different investigated materials, sandstone and whitewood (Figures 1 and 2).

The color changes of given surfaces after application of EOs or SHNPs can be evaluated using CIE 1931 (International Commission on Illumination) color space [32]. In order to calculate the chromaticity coordinates x and y from the reflectivity spectra, we employed the CIE standard daylight illuminant D65 [32], which represents average daylight with the correlated color temperature of 6500 K. Figure 3 shows color space chromaticity diagram with color points plotted for whitewood, whitewood with thyme 50%, and whitewood with SHNPs. The identical data are plotted in CIE $L^*a^*b^*$ color space in Figure S6.

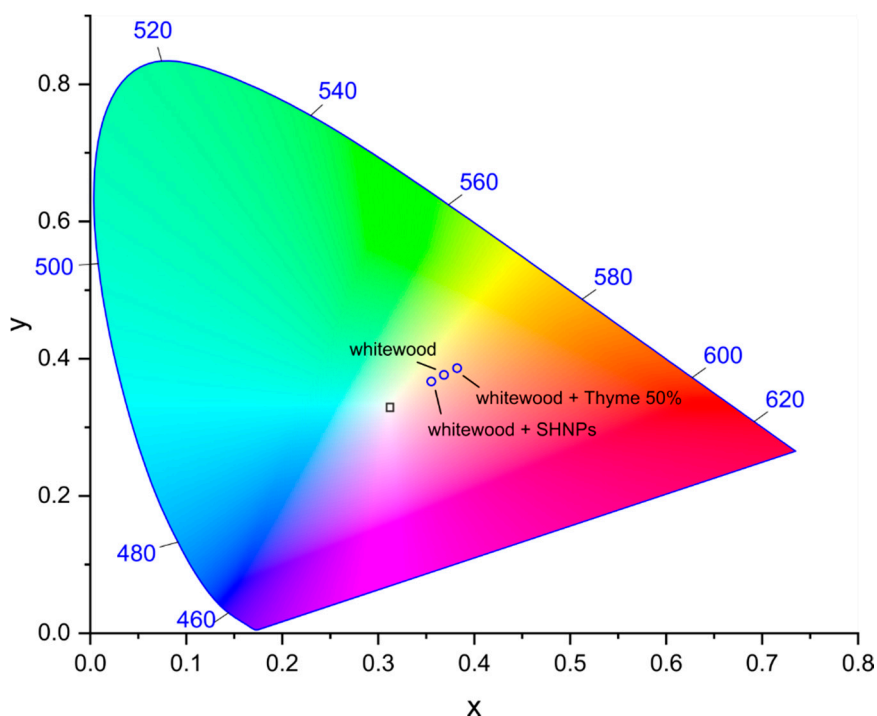


Figure 3. The CIE 1931 color space diagram with the calculated colors for selected whitewood samples (blue circle symbols). The black square symbol shows the ideally reflecting surface.

These samples were selected to illustrate the color changes upon application of EOs and SHNPs. The addition of other EOs and SHNPs on sandstone samples yielded similar results. As can be seen from the reflectivity changes (Figure 1) after application of EOs on whitewood substrates, the lowered reflectivity in the blue-green spectral region results in an overall shift of color appearance towards orange color. On the other hand, the application of SHNPs resulted in enhanced reflectivity in the blue-green spectral part (Figure 1), which makes the surface appearance whiter. It is noteworthy to mention that all color changes proceed along a virtual line in the chromaticity diagram. This is due to the fact that the reflectivity changes of EOs as well as SHNPs are primarily located in the same spectral region. For reference, the ideally reflecting surface with the reflectivity equal to one at all wavelengths is depicted by square black symbol.

Using the digital optical microscope, we were able to exactly localize the fungi on the surface, and thus to calculate the area of their growth (Table 3). We have compared the treated materials with the corresponding control sample without any treatment. Considering the whitewood samples, such comparison confirmed that the fungal growth on their surfaces was negligible. The highest fungal growth along the surface was observed for the samples with 50% of arborvitae oil. Presumably due to a higher density of oil, it showed slower permeation into the wood and partial evaporation of volatile compounds from its surface. These conditions potentially lead to a decreased antifungal activity. This fact was observed also for thyme and oregano oils. However, we have achieved 100% antifungal activity on the whitewood surface coating with 30% of thyme oil. The EO's inhibition of wood-decaying fungi and molds on beech surface was also reported by Pánek et al. [33].

Table 3. The growth area of fungi on assayed surfaces.

	Localized Fungal Area on Surface (mm ²)								
	Whitewood			Sandstone			Paper		
	10%	30%	50%	10%	30%	50%	10%	30%	50%
Arborvitae oil	3.1	3.8	11.8	-	11.9	10.4	22.3	21.5	25.7
Oregano oil	1.5	5	8.1	0.9	4.6	3.8	58.2	40.3	33.2
Thyme oil	0.8	-	3.9	-	2.2	2.7	51.7	32.5	26
SHNPs		0.9			3.5			38	
SHNPs/arborvitae	1.9	1.3	1.3	4.7	20.3	25.4	58.4	36.3	31.9
SHNPs/oregano	4.5	2.9	2.5	-	18.5	23.8	43.1	40.5	19.1
SHNPs/thyme	2.5	2.5	1.4	-	28	22.4	31.3	23.6	16.2
control		28.9			20			89.4	

Note: (-) the fungi area was not recognized.

A different trend was observed for the mixtures of SHNPs and EOs. For the combination of EOs and SHNPs, the antifungal activity was directly linked to the higher content of EOs (Table 3).

Silica-based SHNPs were already used for coating wood [34], but they were not tested to our knowledge against the growth of molds. Surprisingly, our study revealed a limited growth of *A. fumigatus* at only 0.9 mm², when the SHNPs were used alone.

For the protection and consolidation of stone materials and inhibition of their capillary absorption, different silica nanoparticles or hybrid nanocomposites were developed and also tested on cultural heritage objects [35–38]. In our study, the antifungal properties, which were not treated before, were investigated as well. Generally, the antifungal activity on sandstone samples decreased with the increasing percentage of EOs. Significantly better results were achieved using 10% of EOs and 10% of EOs with SHNPs. The 100% antifungal activity on sandstone surface was achieved for the following samples: 10% arborvitae and thyme oils, and 10% oregano and thyme oils with SHNPs. Again, the SHNPs alone were able to limit the growth of *E. xenobiotica*, which spread to an area of 3.5 mm².

The correlation between surface hydrophobicity and antifungal activity was not evident in all treated samples. However, such correlation was displayed on several sandstone samples when they were treated with the mixtures of 10% O/SHNPs or T/SHNPs and no fungal growth was observed, and water contact angles of 108 and 133 were measured, respectively. On paper samples, this correlation was evidenced when the mixture 50% T/SHNPs inhibited the fungal growth (16.2 mm²) and the value 98 for the water contact angle was recorded. In order to explain this discrepancy regarding the coating systems and the treated materials, other studies are necessary, which can be focused on other antifungal compounds of natural origin that perhaps will produce a satisfactory correlation among specific materials, surface hydrophobicity, and antifungal activity.

Some attempts were already performed to use silica SHNPs for the protection of paper [39,40], but as far as we know nobody has paid attention to the preservation against fungal contamination. This study validates that the antifungal activity trend of EOs on paper samples was opposite to the previous sandstone samples. An increasing concentration of EOs reduced the fungal area on the paper surface. This effect is most likely promoted by the paper thickness and its good absorption properties. In this case, the samples with a high concentration of EOs significantly reduced the fungal growth area compared to the control sample.

The fungal penetration into the structure of the coating substrate was monitored by means of cross-sectional cuts in the digital optical microscope. Unfortunately, it was not possible to prepare contamination-free cross-sectional cuts for the paper and sandstone samples due to the thickness and composition of these materials, therefore the fungal penetration was determined only for whitewood samples using wood cleaving techniques. The fungal penetration was measured in the cross-section plane of the wood perpendicular to the substrate surface. In terms of fungal penetration, the results are unambiguous (Table 4, Figure 4); the penetration decreased with the increasing concentration of EOs. The lowest penetration was achieved for SHNPs without EOs. This was assumed because SHNPs

form a hydrophobic barrier. Hence, the conditions for the fungi penetration are worsened. The fungal penetration up to a depth of 315 μm was detected for a mixture of 10% arborvitae and SHNPs. This is a profound difference when compared to the control sample. This may be due to a higher volume of ethanol in 10% EO samples and its rapid evaporation from the surface, together with the volatile active components of EOs. The lower penetration of EOs into the structure of materials can lead to a higher penetration of fungi into the bulk of the materials.

Table 4. Maximum values of fungal penetration into wood samples.

	Penetration Depth (μm) into the Structure of Whitewood		
	10%	30%	50%
Arborvitae oil	127.9	105.4	83.3
Oregano oil	312.0	62.0	62.0
Thyme oil	171.5	69.0	53.0
SHNPs		34.8	
SHNPs/arborvitae	315.0	107.4	53.4
SHNPs/oregano	209.9	117.5	108.8
SHNPs/thyme	277.3	156.1	125.9
control		138	

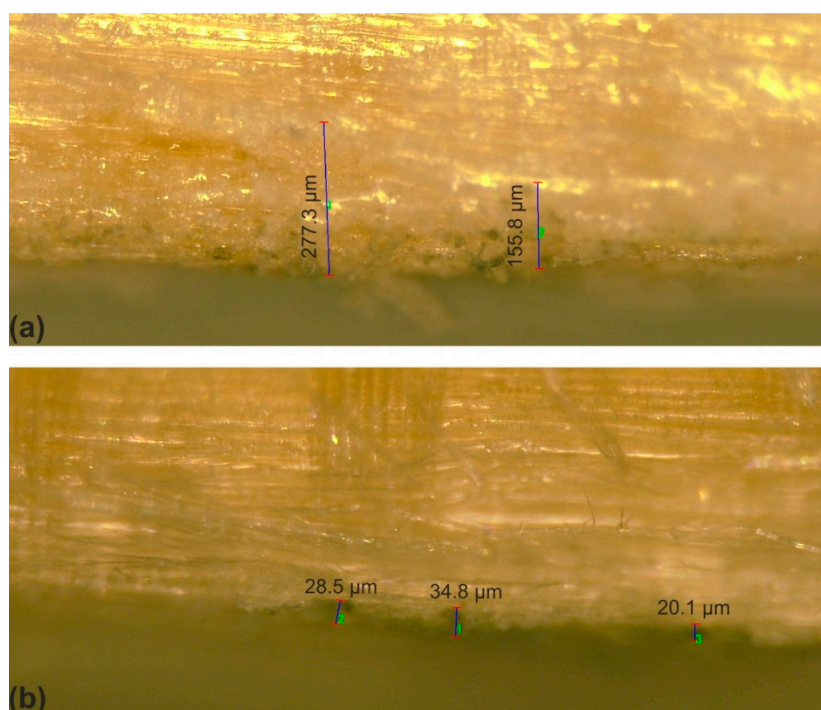


Figure 4. *A. fumigatus* penetration into wood structure treated with 10% of thyme and SHNPs (a) and SHNPs exclusively (b). The numbers (1, 2, 3) indicate the order of penetration depth (μm) into the structure of the whitewood.

On the whitewood surface coated with 50% of EOs, it was observed that the largest localized fungal area corresponds to the lowest fungal penetration depth into the structure.

4. Conclusions

In terms of material protection, the use of EOs as potential surface preservation coadjuvants is highly promoted. Our results demonstrated that the antifungal effect of EOs alone or in combination with SHNPs depends on the type of EOs and on the type of targeted material as well. EO/SHNP combinations are more suitable for wood protection, although the *A. fumigatus* was able to penetrate

inside the model samples. In addition, it is necessary to emphasize that a satisfactory hydrophobicity of treated wood is guaranteed only for a low concentration of EOs.

The same situation was also displayed for the sandstone; in fact, the use of 10% EOs (thyme or oregano) with SHNPs conferred a total protection of the tested material. Moreover, it is possible to consider the use of SHNPs alone; interesting results were obtained regarding the inhibition of fungal growth in both wood and sandstone, with the lowest value of fungal penetration in wood.

The color change of the material after application of EOs and SHNPs was at an acceptable level, which is important, especially for the surfaces that require the preservation of original color appearance. Generally, the application of studied EOs onto surfaces shifts the color saturation towards orange-yellow. On the contrary, the application of SHNPs shifts the color towards white due to enhanced Rayleigh scattering in the blue part of the visible spectrum.

This investigation has demonstrated a possible application of SHNPs, alone or with EOs, for preservation of interior building materials or furniture against the colonization of molds. The use during the experimentation of a high fungal concentration, which generally is not possible to encounter in a normal indoor environment, is further evidence of their antifungal properties.

In the future, it would be worth to assay their inhibition effect on the growth of specific microbial communities.

Supplementary Materials: The following are available online at <http://www.mdpi.com/2079-6412/9/3/176/s1>. Figure S1: Illustrative images of untreated and treated samples affected by fungal growth. A, O, T mean arborvitae, oregano, and thyme, respectively. Figure S2: Scheme of reflectance measurement in diffuse setting. Figure S3: Disc diffusion assay of *Exophiala* sp. on petri dishes. Figure S4: Disc diffusion assay of *A. fumigatus* on petri dishes. Figure S5: The water contact angle measurements of various samples of whitewood, sandstone, and paper substrate. A, O, T mean arborvitae, oregano, and thyme essential oils, respectively. Figure S6: Color changes of whitewood samples after application of SHNPs and 50% thyme EO encoded in CIE L*a*b* color space. The color differences E^*_{ab} are given in the upper-right corner.

Author Contributions: Synthesis of superhydrophobic nanoparticles, physical measurements, Monika Benkovičová and Peter Šiffalovič. Isolation and cultivation of fungal strains, disc diffusion assay on petri dishes, Zuzana Kisová and Mária Bučková. Funding Acquisition and supervision, Domenico Pangallo and Eva Majková.

Funding: This work was supported by VEGA Agency with the projects 2/0061/17 and 2/0059/19. The financial support of the Slovak Research and Development Agency, project no. APVV-15-0641, is acknowledged too.

Conflicts of Interest: The authors declare no conflict of interest.

References

1. Carlborg, C.F.; van der Wijngaart, W. Sustained Superhydrophobic Friction Reduction at High Liquid Pressures and Large Flows. *Langmuir* **2011**, *27*, 487–493. [CrossRef] [PubMed]
2. Nosonovsky, M.; Bhushan, B. Roughness-Induced Superhydrophobicity: A Way to Design Non-Adhesive Surfaces. *J. Phys. Condens. Matter* **2008**, *20*, 225009. [CrossRef]
3. Nosonovsky, M.; Bhushan, B. Hierarchical Roughness Makes Superhydrophobic States Stable. *Microelectron. Eng.* **2007**, *84*, 382–386.
4. Verplanck, N.; Coffinier, Y.; Thomy, V.; Boukherroub, R. Wettability Switching Techniques on Superhydrophobic Surfaces. *Nanoscale Res. Lett.* **2007**, *2*, 577–596. [CrossRef]
5. Šiffalovič, P.; Jergel, M.; Benkovičová, M.; Vojtko, A.; Nádaždy, V.; Ivančo, J.; Bodík, M.; Demydenko, M.; Majková, E. Towards New Multifunctional Coatings for Organic Photovoltaics. *Sol. Energy Mater. Sol. Cells* **2014**, *125*, 127–132. [CrossRef]
6. Teisala, H.; Tuominen, M.; Kuusipalo, J. Adhesion Mechanism of Water Droplets on Hierarchically Rough Superhydrophobic Rose Petal Surface. *J. Nanomater.* **2011**, *2011*, 33. [CrossRef]
7. Daouk, R.K.; Dagher, S.M.; Sattout, E.J. Antifungal Activity of the Essential Oil of *Origanum syriacum* L. *J. Food Prot.* **1995**, *58*, 1147–1149. [CrossRef]
8. Gakuubi, M.M.; Maina, A.W.; Wagacha, J.M. Antifungal Activity of Essential Oil of *Eucalyptus camaldulensis* Dehnh. against Selected *Fusarium* Spp. *Int. J. Microbiol.* **2017**, *2017*, 8761610. [CrossRef] [PubMed]

9. Puškárová, A.; Bučková, M.; Kraková, L.; Pangallo, D.; Kozics, K. The Antibacterial and Antifungal Activity of Six Essential Oils and Their Cyto/Genotoxicity to Human HEL 12469 Cells. *Sci. Rep.* **2017**, *7*, 1–11. [[CrossRef](#)] [[PubMed](#)]
10. Boskovic, M.; Zdravkovic, N.; Ivanovic, J.; Janjic, J.; Djordjevic, J.; Starcevic, M.; Baltic, M.Z. Antimicrobial Activity of Thyme (*Tymus vulgaris*) and Oregano (*Origanum vulgare*) Essential Oils against Some Food-Borne Microorganisms. *Procedia Food Sci.* **2015**, *5*, 18–21. [[CrossRef](#)]
11. Mohareb, A.; Badawy, M.E.I.; Abdelgaleil, S.A.M. Antifungal Activity of Essential Oils Isolated from Egyptian Plants against Wood Decay Fungi. *J. Wood Sci.* **2013**, *59*, 499–505. [[CrossRef](#)]
12. Han, X.; Parker, T.L. Arborvitae (*Thuja plicata*) Essential Oil Significantly Inhibited Critical Inflammation- and Tissue Remodeling-Related Proteins and Genes in Human Dermal Fibroblasts. *Biochim. Open* **2017**, *4*, 56–60. [[CrossRef](#)] [[PubMed](#)]
13. Santoro, G.F.; Das Graças Cardoso, M.; Guimarães, L.G.L.; Salgado, A.P.S.P.; Menna-Barreto, R.F.S.; Soares, M.J. Effect of Oregano (*Origanum vulgare* L.) and Thyme (*Thymus vulgaris* L.) Essential Oils on *Trypanosoma cruzi* (Protozoa: Kinetoplastida) Growth and Ultrastructure. *Parasitol. Res.* **2007**, *100*, 783–790. [[CrossRef](#)] [[PubMed](#)]
14. Souza, E.L.; Stamford, T.L.M.; Lima, E.O.; Trajano, V.N. Effectiveness of *Origanum vulgare* L. Essential Oil to Inhibit the Growth of Food Spoiling Yeasts. *Food Control* **2007**, *18*, 409–413. [[CrossRef](#)]
15. Magyar, D.; Vass, M.; Li, D. *Biology of Microfungi*; Li, D.-W., Ed.; Springer International Publishing: Cham, Switzerland, 2016.
16. Carmo, E.S.; Lima, E.D.O.; De Souza, E.L. The Potential of *Origanum vulgare* L. (Lamiaceae) Essential Oil in Inhibiting the Growth of Some Food-Related Aspergillus Species. *Braz. J. Microbiol.* **2008**, *39*, 362–367. [[CrossRef](#)] [[PubMed](#)]
17. Mith, H.; Duré, R.; Delcenserie, V.; Zhiri, A.; Daube, G.; Clinquart, A. Antimicrobial Activities of Commercial Essential Oils and Their Components against Food-Borne Pathogens and Food Spoilage Bacteria. *Food Sci. Nutr.* **2014**, *2*, 403–416. [[CrossRef](#)] [[PubMed](#)]
18. Hatakka, A.; Hammel, K.E. Fungal Biodegradation of Lignocelluloses. *Ind. Appl.* **2011**, 319–340.
19. Kraková, L.; Chovanová, K.; Selim, S.A.; Šimonovičová, A.; Puškárová, A.; Maková, A.; Pangallo, D. A Multiphasic Approach for Investigation of the Microbial Diversity and Its Biodegradative Abilities in Historical Paper and Parchment Documents. *Int. Biodeterior. Biodegrad.* **2012**, *70*, 117–125. [[CrossRef](#)]
20. Nieminen, S.M.; Kärki, R.; Auriola, S.; Toivola, M.; Laatsch, H.; Laatikainen, R.; Hyvärinen, A.; von Wright, A. Isolation and Identification of Aspergillus Fumigatus Mycotoxins on Growth Medium and Some Building Materials Isolation and Identification of Aspergillus Fumigatus Mycotoxins on Growth Medium and Some Building Materials. *Appl. Environ. Microbiol.* **2002**, *68*, 4871–4875. [[CrossRef](#)] [[PubMed](#)]
21. Kumar, M.; Verma, R.K. Fungi Diversity, Their Effects on Building Materials, Occupants and Control—A Brief Review. *J. Sci. Ind. Res.* **2010**, *69*, 657–661.
22. Urzi, C. Microbial Deterioration of Rocks and Marble Monuments of the Mediterranean Basin: A Review. *Corros. Rev.* **2004**, *22*, 441–457. [[CrossRef](#)]
23. Wiktor, V.; De Leo, F.; Urzi, C.; Guyonnet, R.; Grosseau, P.; Garcia-Diaz, E. Accelerated Laboratory Test to Study Fungal Biodeterioration of Cementitious Matrix. *Int. Biodeterior. Biodegrad.* **2009**, *63*, 1061–1065. [[CrossRef](#)]
24. De Leo, F.; Cardiano, P.; De Carlo, G.; Lo Schiavo, S.; Urzi, C. Testing the Antimicrobial Properties of an Upcoming “Environmental-Friendly” Family of Ionic Liquids. *J. Mol. Liq.* **2017**, *248*, 81–85. [[CrossRef](#)]
25. La Russa, M.F.; Macchia, A.; Ruffolo, S.A.; De Leo, F.; Barberio, M.; Barone, P.; Crisci, G.M.; Urzi, C. Testing the Antibacterial Activity of Doped TiO₂ for Preventing Biodeterioration of Cultural Heritage Building Materials. *Int. Biodeterior. Biodegrad.* **2014**, *96*, 87–96. [[CrossRef](#)]
26. Ruffolo, S.A.; De Leo, F.; Ricca, M.; Arcudi, A.; Silvestri, C.; Bruno, L.; Urzi, C.; La Russa, M.F. Medium-Term in Situ Experiment by Using Organic Biocides and Titanium Dioxide for the Mitigation of Microbial Colonization on Stone Surfaces. *Int. Biodeterior. Biodegrad.* **2017**, *123*, 17–26. [[CrossRef](#)]
27. Scheerer, S.; Ortega-Morales, O.; Gaylarde, C. *Chapter 5 Microbial Deterioration of Stone Monuments—An Updated Overview*, 1st ed.; Elsevier B.V. Inc.: Amsterdam, The Netherlands, 2009; Volume 66.
28. Sadiki, M.; Barkai, H.; Saad, I.K. The Effect of the Thymus Vulgaris Extracts on the Physicochemical Characteristics of Cedar Wood Using Angle Contact Measurement. *J. Adhes. Sci. Technol.* **2014**, *28*, 1925–1934.

29. Van Oss, C.J.; Ju, L.; Chaudhury, M.K.; Good, R.J. Estimation of the Polar Parameters of the Surface Tension of Liquids by Contact Angle Measurements on Gels. *J. Colloid Interface Sci.* **1988**, *128*, 313–319. [[CrossRef](#)]
30. Vogler, E.A. Structure and Reactivity of Water at Biomaterial Surfaces. *Adv. Colloid Interface Sci.* **1998**, *74*, 69–117. [[CrossRef](#)]
31. Law, K.-Y. Definitions for Hydrophilicity, Hydrophobicity, and Superhydrophobicity: Getting the Basics Right. *Phys. Chem. Lett.* **2014**, *5*, 686–688. [[CrossRef](#)] [[PubMed](#)]
32. Ohta, N.; Robertson, A.R. *Colorimetry: Fundamentals and Applications*; John Wiley & Sons Ltd.: West Sussex, England, 2005.
33. Panek, M.; Reinprecht, L.; Hulla, M. Ten Essential Oils for Beech Wood Protection—Efficacy Against Wood-Destroying Fungi and Moulds, and Effect on Wood Discoloration. *BioResources* **2014**, *9*, 5588–5603. [[CrossRef](#)]
34. Wang, C.; Zhang, M.; Xu, Y.; Wang, S.; Liu, F.; Ma, M.; Zang, D.; Gao, Z. One-Step Synthesis of Unique Silica Particles for the Fabrication of Bionic and Stably Superhydrophobic Coatings on Wood Surface. *Adv. Powder Technol.* **2014**, *25*, 530–535. [[CrossRef](#)]
35. de Ferri, L.; Paolo, P.; Lorenzi, A.; Montenero, A.; Salvioli-mariani, E. Study of Silica Nanoparticles—Polysiloxane Hydrophobic Treatments for Stone-Based Monument Protection. *J. Cult. Herit.* **2011**, *12*, 356–363. [[CrossRef](#)]
36. Aslanidou, D.; Karapanagiotis, I.; Panayiotou, C. Tuning the Wetting Properties of Siloxane-Nanoparticle Coatings to Induce Superhydrophobicity and Superoleophobicity for Stone Protection. *Mater. Des.* **2016**, *108*, 736–744. [[CrossRef](#)]
37. Facio, D.S.; Ordoñez, J.A.; Gil, M.L.A.; Carrascosa, L.A.M.; Mosquera, M.J. Combining SiO₂ Composite and Fluorinated Alkoxysilane: Application on Decayed Biocalcareous Stone from an 18th Century Cathedral. *Coatings* **2018**, *8*, 170. [[CrossRef](#)]
38. Frigione, M.; Lettieri, M. Novel Attribute of Organic—Inorganic Hybrid. *Coatings* **2018**, *8*, 319. [[CrossRef](#)]
39. Li, K.; Zeng, X.; Li, H.; Lai, X. Fabrication and Characterization of Stable Superhydrophobic Fluorinated-Polyacrylate/Silica Hybrid Coating. *Appl. Surf. Sci.* **2014**, *298*, 214–220. [[CrossRef](#)]
40. Teisala, H.; Tuominen, M.; Kuusipalo, J. Superhydrophobic Coatings on Cellulose-Based Materials: Fabrication, Properties, and Applications. *Adv. Mater. Interfaces* **2014**, *1*, 1300026. [[CrossRef](#)]



© 2019 by the authors. Licensee MDPI, Basel, Switzerland. This article is an open access article distributed under the terms and conditions of the Creative Commons Attribution (CC BY) license (<http://creativecommons.org/licenses/by/4.0/>).